Proceedings of Building Simulation 2011:
12th Conference of International Building Performance Simulation Association, Sydney, 14-16 November.

VALIDATION OF AN ACTIVE CHILLED BEAM DESIGN FOR A HEALTHCARE FACILITY

Nick Devlin
AECOM, Perth, Australia
nick.devlin@aecom.com
May 2011

ABSTRACT

Conventional air-conditioning methods in hospitals have often involved air-recycling and indefinite pressure regimes, which increase cross-infection risk. Poor comfort conditions and indoor air quality (IAQ) have also been issues. These were major considerations in the design of the $1.8B Fiona Stanley Hospital.

Active chilled beams (ACBs) were selected for the wards. ACBs provide constant volume air supply, which allows air paths to be tightly controlled, they use 100% outside air, which prevents recycling of air between different rooms, and they provide individual room temperature control. However, comfort, IAQ and condensation were all concerns.

Computational Fluid Dynamics (CFD) simulation and full-scale prototype testing were used to verify the decision to use ACBs.

The findings of this paper support the decision to use an ACB solution, and highlight the importance of accurate modelling and prototyping.

INTRODUCTION

Heating, ventilating and air-conditioning (HVAC) systems for healthcare projects are required to satisfy a wider variety of functions than many other building applications. The system must provide a safe and comfortable environment for immuno-compromised, weakened or infectious patients, satisfy environmental quality requirements for staff and other building occupants, it must be economically viable, reliable, maintainable and energy efficient. Furthermore, changing legislation, standards and client expectations result in a dynamic ‘design landscape’ for building services engineers. For example, Smith et al (2010) used simulation software to estimate the energy reduction for a hospital designed to Building Code of Australia (BCA) 2010 as opposed to BCA 2009. The results showed compliance with BCA 2010 would require an energy performance improvement in the order of 15%. An example of a changing healthcare design standard is NSW TS11 Healthcare Guidelines, which is currently being revised. It is expected that greater emphasis will be placed on hygiene and ‘greener’ healthcare facilities in the new guidelines.

Health and infection control were the most critical criteria to address in the design of the Fiona Stanley Hospital and significant research was carried out into airborne cross-infection risk. At the time, calls were being made to reduce hospital-acquired infection rates (Australian Health Insurance Association, 2007). A HVAC system, which would provide 100% outside air and no recycling, was decided upon.

The system options were reduced to the following:

- conventional constant volume;
- displacement ventilation; and
- ACBs.

ACBs were selected as they offered the following:

- 100% outside air and no recycling of air between rooms;
- definite control of airflow direction;
- individual room temperature control;
- reduced plant space requirements; and
- best overall 30 year life cycle cost.

ACBs have been widely and successfully used in commercial applications (Roth et al., 2007), but less commonly used in the healthcare sector. As the system would be used in approximately 800 wards, CFD analysis was used to allow the design to proceed with greater confidence. Prior to construction, a full-scale prototype room was used to test the ACB performance under differing and transient conditions.

WARD AIRFLOW REGIME

To reduce the risk of cross-infection, the wards were designed to maintain a direction of airflow from the adjoining corridor into the ward. See Figure 2.

HOW AN ACB WORKS

An ACB works by receiving pre-conditioned, dehumidified primary air from a separate air handling unit (AHU). The primary air is forced through nozzles inside the ACB, which causes room air to be induced into the primary air stream. A secondary coil is imposed in the path of this induced room air causing the secondary air to be sensibly cooled, mixed with the primary air and delivered to the room.

Figure 1

How an ACB works

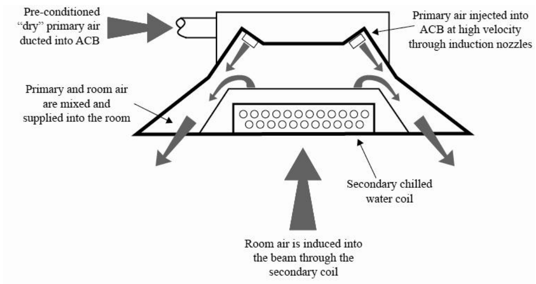

CFD SIMULATION METHODOLOGY

A CFD model of a typical ward under part-load conditions was generated and tested. The model was constructed primarily using the 'CFD-ACE' software package produced by ESI Group. The geometry was generated in 'CFD-GEOM', and meshed using 'Harpoon', the simulation was processed using 'CFD-ACE', and post-processed using 'CFD-VIEW'. The model was based upon idealistic geometrical constraints available at the time of development, while boundary conditions and thermal and occupancy loads were based on estimated profiles.

The ward configuration consisted of a single ACB unit providing 45L/s of primary air into the ward space with a profile, which consisted of a hospital bed, a patient and two other occupants. The boundary conditions for the heat load and flow rates into the ward space are summarised in the table below.

Table 1

Modelled heat loads

LOAD TYPE	**HEAT LOADS**	
	SENSIBLE (W)	**LATENT (W)**
People	190	133
Lights	135	0
Equipment	130	0
Glazing	102	0

The simulation used a steady-state solver, which assumes the flow domain features temporarily steady flow. A Reynolds-Averaged Navier Stokes (RANS) solver was used for the analysis, with a standard k-epsilon turbulence model introduced to account for the nature of the flow-field. Mesh refinement was introduced in areas of complicated geometry to capture the intricate flow structures which are produced within regions close to obstructions. Larger cells were used in areas where there were no geometrical features to produce a more time, and hence cost effective analysis. The effect of gravity was also included to account for the effects of fluid buoyancy. The total number of cells used within the domain was 2.25 million, with the model solving the flow field, heat transfer and turbulence.

A temperature of 300K (27°C) was applied to all volumes within the model as an initial condition, with a reference pressure of 101.325kPa.

The model was run with a maximum of 1500 iterations, with a convergence criterion of $1 \quad 10^{-4}$ and with a minimum residual value of $1 \quad 10^{-18}$.

Graphical plots were generated indicating air temperatures and velocities to gain an understanding of comfort conditions, and a 'particle stream trace' to identify any potential poorly ventilated regions of the room.

FULL-SCALE PROTOTYPE ROOM TEST METHODOLOGY

Testing was undertaken at an air distribution laboratory in South Australia (Dadanco, 2011). The actual room geometry and dimensions of the ward, in-room objects and ensuite were replicated. The room was served by an AHU capable of controlling the primary air temperature and flow rate. It was also equipped with lighting similar to that of the planned ward, thermal mannequins which were used to mimic occupant's heat loads, and a 'climate panel' (CP) to simulate the heat load/loss through the facade. The test room parameters are given in the table below.

Table 2

Test parameters

PARAMETER	**VALUE/ UNIT**
Room temperature	23°C cooling, 20°C heating
Chilled water supply temperature & flow rate to the ACB	14°C, 0.04kg/s
Primary air supply temperature	11.4°C cooling, 24°C heating
Primary air flow rate	45L/s
ACB plenum static Pressure	148Pa
Total cooling/ heating capacity	1197W clg, 150W htg
Primary air cooling/ heating capacity	633W clg @23°C room, 150W htg @20°C room
ACB secondary cooling capacity @ 23°C room	564W cooling 23°C Room, heating - nil

The test room was equipped with the following capabilities to monitor the actual room conditions on a uniform grid at 0.2m, 0.6m, 1.2m and 1.7m above floor level (see Figure 7 and tables 8, 9 & 10):

- air velocity;
- air dry bulb temperature;
- room mean radiant temperature; and
- air humidity.

The above monitoring was achieved through the use of a moveable stand. During each test, the stand was moved to each position on the grid. A settling time of 2 minutes was allowed prior to taking readings at each point.

The following data was also logged to ensure the validity of the test results:

- chilled water flow and return temperature;
- chilled water flow rate;
- mean chilled water temperature;
- primary supply air temperature;
- ACB plenum static pressure;
- 2 room temperature static probes; and
- mean room temperature.

Before all tests, the air and water systems were commissioned. The ACB plenum was set to the correct pressure, and hence flow rate using a variable speed fan at the AHU. The water flow rate was adjusted using a commissioning valve in the pipe work supplying water to the ACB. The ultrasonic flow rate displayed by the Building management System (BMS) was compared with the flow measured across the orifice of the commissioning valve serving the chilled beam. The recorded values showed negligible error.

BS EN 15116:2008 was not specifically followed as this test was project specific, however the standard does specify the limits of what can be deemed 'steady-state' as shown in the following table. These values were adhered to in the steady-state tests:

Table 3

Maximum one-hour standard deviation

Room temperature	0.05K
Mean chilled water temperature	0.05K
Primary air supply temperature	0.2K

The following tests were carried out in steady-state:

Test 1: Part-load cooling – The prototype room was tested with the same part-load test parameters as the CFD model, and the conditions in the space were recorded. See Table 1 for details of heat load allowances.

Test 2: Full load cooling – the ACB system was tested under steady-state conditions to peak design cooling conditions as per Table 4 and the conditions in the space were recorded.

Table 4

Test 2 Design cooling loads

LOAD TYPE	HEAT LOADS	
	SENSIBLE (W)	LATENT (W)
People	280	200
Lights	135	0
Equipment	200	0
Glazing	583	0

Test 3: Full load heating – the airside heating was tested under winter conditions and a room set-point of 20°C and loads as per the below table, and the conditions in the space recorded.

Table 5

Test 3 Design heating loads

LOAD TYPE	HEAT LOADS	
	SENSIBLE (W)	LATENT (W)
Patient	50	N/A
Glazing	-200	0

For all the steady-state tests, an artificial heat load that equated to the predicted design heat gains in the internal space was applied using thermal mannequins (see Figure 3) and the lighting. Simultaneously, the systems that provide water to the AHU and the ACB, and water to the CPs for the facade load were activated. In each test, the system as a whole was left to settle while the BMS made the necessary adjustments to achieve the desired water supply temperatures and flow rates.

Figure 3

Thermal mannequins and test equipment

Table 6

Equipment modes for steady-state tests

TEST	PRIMARY AHU MODE	ACB MODE	CP MODE	HEAT LOADS
1	Cooling	Off	Warm	On
2	Cooling	Cooling	Warm	On
3	Heating	Off	Cold	On

The above table indicates the mode of each of the components for each of the steady-state tests. Under each test, once the room was in a stabilised condition that satisfied the design parameters, data was extracted from the BMS.

The following transient tests were carried out:

Test 4: Cooling recovery – Using the same conditions used for Test 2, the temperature of the test cell was allowed to rise to 26.7°C by stopping the pump that supplied chilled water to the ACB. Once 26.7°C was reached, the chilled water pump was restarted and the time required to return the space to 23°C was recorded.

Test 5: Condensate fail

Ultrasonic humidifiers located within the room were switched on to supply moisture to the test room. To simulate a likely scenario, the humidifiers were placed at the location of the ensuite door to simulate moisture from the ensuite shower rather than using moisture in the duct. The humidifiers were controlled by the BMS system to regulate the room at a selected humidity level. The test began with an initial value being entered into the system, which operated the humidifiers at full capacity until the BMS received a signal to indicate that the room was at the nominated humidity condition. The humidifiers were then switched off and on automatically based on a control band. The cycle of driving the system to a known humidity and observing the outcome was repeated by increasing the preset humidity values at regular intervals until condensation was observed at the ACB. At every control point, the room was held in a constant moisture state while observations were made and monitoring points were logged.

RESULTS

Test 1: Part-load cooling

Plots of the CFD predicted temperature and velocities under part-load conditions can be seen in table 8. The CFD model predicted uniform temperatures across the space (<1K gradient was achieved almost throughout the room). See Figure 4. It also predicted very low velocities (<0.1m/s around the patient). See Figure 5.

Figure 4

Temperature plot

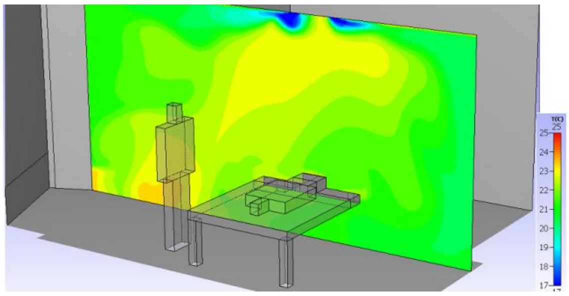

Figure 5

Velocity plot

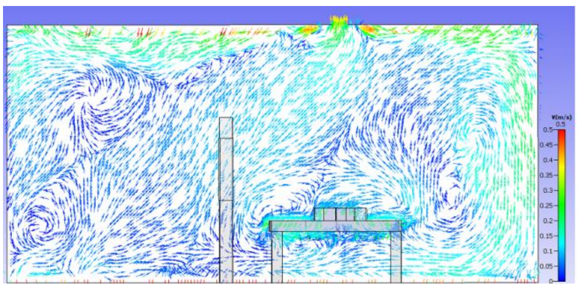

Table 9 indicates temperature and velocity scans for the prototype room. The recorded air temperature readings across the prototype space showed a high level of uniformity and consistency with the CFD results (see table 10). The temperature differential between the highest and lowest recorded temperatures was 0.7K and the highest vertical temperature gradient was 0.3K. The results show that the temperature uniformity of the prototype room was greater than the CFD model prediction.

Table 8 shows that the CFD model predicted low velocities throughout the room, particularly in the occupied zone. The recorded values are lower than the recommended ASHRAE 55:1992 velocity comfort limits. Table 9 shows the much higher velocities recorded during the prototype test. The recorded values are generally within ASHRAE 55:1992 comfort limits. The comparison in table 10 shows that there is significant error between the CFD velocity predictions and the measured velocities. An average percentage error in the order of 100% was recorded, and isolated occurrences of errors in excess of 400% were recorded.

It should be noted that in all the prototype tests, the mean radiant temperature (MRT) was recorded, as well as the air temperature. The difference between the air temperature and MRT readings was found to be negligible due to only a small section of well protected facade opening onto the room. Relative humidity was also recorded and it remained steady at 35%RH in the room.

Air stagnation is one concern in infection control. The CFD model also provided particle stream tracing, which provides an indication of air change effectiveness. Figure 6 shows the path of twenty tracer particles that were released from the outlets of the ACB. The cool air jet clings to the ceiling due to the Coandă effect. This jet penetrates to the walls upon which the cooler air falls and becomes well mixed with the air inside the ward. This was not replicated in a format that could be measured in the prototype test, but tracer gas test footage appears to support this result.

Figure 6

Particle stream trace

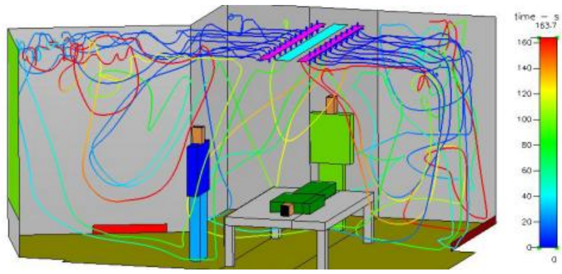

Test 2: Full load cooling

Recorded results show that conditions recorded on the right hand side of the room were generally well below 0.25m/s, although there was a velocity reading at 0.2m above floor height that exceeded 0.25m/s. The left hand side of the room also had some instances of velocities at 0.2m (ankle height) that exceed 0.3m/s.

The scans show that temperature uniformity across the space was of a high order even at full design load. The gradient between the highest and lowest recorded value was 0.9K and the maximum gradient recorded between ankle and head height was 0.7K.

Humidity was recorded at a steady 37%RH throughout the test.

Test 3: Full load heating

Air movement recorded in the test space was generally within accepted margins regarding occupant comfort (<0.25m/s). There was an area with 2 elevated velocity readings adjacent the glazing side of the bed. The peak velocities exceeded those recorded under full cooling.

The highest recorded vertical temperature gradient between ankle and head was measured at 0.4K. The variance across the test space between the maximum and minimum recorded temperatures was 0.8K. This differential is consistent with provision of acceptable occupant comfort.

Humidity was recorded at a steady 59%RH throughout the test, however, this is not representative of actual expected winter conditions in Perth.

Test 4: Cooling recovery

The below table shows the time of recovery for the system after the temperature was allowed to drift out to 26.7°C by switching off the chilled water.

Table 7

Time for room temperature to return to 23°C

EVENT	RECOVERY
Chilled water on at 26.7°C	0 mins
Room Mean Temp 26°C	3 mins
Room Mean Temp 25°C	8 mins
Room Mean Temp 24°C	18 mins
Room Mean Temp 23.5°C	29 mins
Room Mean Temp 23°C	56 mins

The test showed the recovery time to achieve a room temperature of 23°C was 56 minutes. However, it took approximately one third of this time to recover to 24°C.

Test 5: Condensate fail

Figure 8 shows the chilled water temperature minus the room dew-point temperature.

During the initial hour the dew point was controlled at around 12°C to replicate the dew point at 23°C with 50%RH. The secondary coil was observed to be dry, as would be expected.

After approximately one and a half hours of dew-point conflict, the first signs of moisture where the coldest water enters the coil were detected. The moisture present was negligible at this stage.

After another hour had passed, misting had spread across the fins from the coldest part of the ACB to the periphery of the heat exchanger. Evidence of the moisture film combining into small droplets was visible.

Almost one hour later, the coil had reached a point where the fins at the supply end of the coil were beginning to fill with moisture as large droplets formed. A single droplet was observed to fall from the ACB.

DISCUSSION

Test 1: Part load cooling

The CFD model predicted temperatures under part-load conditions consistent with a comfortable environment. This is supported by the results from the prototype room, which actually improves on the temperature uniformity prediction. An indicator, when considering temperature variance in an occupied space is the differential permitted in BS EN ISO 7730: 2005 for the vertical temperature gradient between ankle and head height. To achieve the highest rating, Category A, the gradient should be less than 2K (Dadanco, 2011). Hence, it is quite clear, that the air temperature differentials recorded in this exercise are consistent with appropriate comfort conditions for occupants.

The higher velocities recorded in the prototype test go some way to explaining the greater uniformity of temperature, as the air mixing within the room would improve due to greater turbulence. Notwithstanding the increased velocities, the actual average velocity below 1.8m height was in the order of 0.15m/s, which is satisfactory, and velocities that exceeded 0.25m/s were generally away from the patient bed and only at low height (0.2m above the floor in all cases). ASHRAE 55:1992 suggests that mean air velocities should be 0.15-0.25m/s in 23°C spaces.

The discrepancy in the velocity prediction points to deficiencies in the modelling of the supply air delivery into the room. Due to time and processing constraints, the ACB was modelled at steady-state using simple slots with fixed face velocities.

However, as described previously, in ACBs, nozzles are used in the delivery of air through a low resistance curved profile. The actual air delivery characteristics and velocity profiles were therefore not accurately CFD modelled and this has resulted in significant error. Jennings (2010) investigated the limitations of steady-state CFD models comparing RANS simulation results against empirically derived data, finding error in aspects of the computational results. This risk of inaccuracy should be addressed in future computational models of airflow in critical applications.

Although the particle stream trace' test in the CFD model was not replicated in the prototype test objectively, given that the velocity, and hence air mixing, have been shown to be increased in the prototype test, it is likely that the 'real world' scenario will be an improvement on the CFD predictions with enhanced air change effectiveness.

The room conditions recorded in the prototype test were used as input parameters to calculate the 'Public Mean Vote' (PMV), developed by Fanger (Charles, 2003). The PMV metric, when calculated in accordance with BS EN ISO7730-2005, showed that an inactive patient wearing light clothing in a room at 23°C air temperature and 23°C MRT, with 35%RH, and velocity at 0.2m/s, would suffer discomfort and would feel the space to be too cold. In order to address this issue the patient would need to have access to thermal blankets in order to compensate for any perceived discomfort. On the other hand, there is a potential energy benefit in that the room temperature could be drifted out to a much higher temperature. The PMV metric predicts that a room temperature in the order of 27°C could be provided for a patient whilst satisfying, or even improving comfort requirements. This opens up opportunities for energy saving. However, regardless of the selected room temperature, the patient's comfort will be heavily contingent on personal adjustment of bedclothes. A balance will also need to be found between patient and staff comfort requirements, which will be quite different due to clothing types and activity levels.

Test 2: Full load cooling

The uniformity of temperature and overall low velocities recorded in the space indicate that comfort conditions will be favourable in the room if the room set point is selected correctly.

There is an instance of a velocity reading exceeding 0.25m/s. However, the reading taken was only 570mm from the wall, and it is most likely this location will only be used for transient activities, so is very unlikely to cause discomfort.

One side of the room had velocities at 0.2m above floor level that exceeded 0.3m/s. This is thought to be caused by the geometry of the ensuite. Due to the low height of the velocity occurrence and its position, this is unlikely to create a comfort issue for occupants.

Based on the BS EN ISO7730:2005, a temperature <2K from ankle to head height would be classified category A, the highest rating. The maximum ankle to head height gradient recorded was 0.7K. Clearly, the results surpass the category A requirements.

Test 3: Full load heating

Velocity readings were generally below 0.25m/s. The likely reason for the increased velocity readings adjacent the facade is that the air stream discharged by the ACB combined with the downdraught generated by natural convection at the cold window surface.

There was initial concern that the warm supply air would not fully penetrate the occupied zone, which could create an uncomfortable temperature gradient for the occupants. However, the results have shown a high level of temperature uniformity.

The PMV metric was applied to the values recorded in the heating test. It showed that an inactive patient wearing light clothing in a room at 20°C air temperature and 20°C MRT, with 30%RH, and velocity at 0.2m/s, would suffer a great deal of discomfort, and would feel the space to be too cold. In the actual design, there is sufficient spare heating capacity to reset the room set-point to a higher temperature. This will improve comfort conditions and reduce the effect of the downdraught at the window. Again, notwithstanding any favourable set-point adjustments, acceptable comfort for the patient will likely only be achieved through personal adjustment of bedclothes.

Test 4: Cooling recovery

It is clear that the temperature recovery time was close to one hour. However, the initial temperature pull-down to 25°C is rapid (8 minutes) and is therefore considered an acceptable response time. The slowing in the rate of recovery as the room set-point is approached is expected and is a function of the log mean temperature differential between the room temperature and the ACB coil temperature.

Test 5: Condensate fail

The data clearly shows that under certain conditions ACBs can continue to operate for a substantial period of time without occupant discomfort should a loss of moisture control occur in the building.

The concern that the theoretical dew point rising above the chilled water supply temperature will result in rapid in-room 'raining' was shown to be unfounded. A room dew-point temperature in the order of 1.5°C higher than the entering water temperature failure took over three hours before dripping occurred. This result is significant, as ACBs will be positioned above patient beds. Failsafe features are built into the design in order to prevent condensation, however, the results show the controls can be relaxed somewhat, which will allow opportunities for primary air temperature reset, resulting in significant energy savings.

CONCLUSION

The modelling and testing showed the ACB system to be an appropriate solution for the hospital wards. The constant volume air supply method, pressure regimes and direction of airflow associated with the ACBs should reduce airborne cross-infection risk. ACBs offer an efficient method of delivering 100% outside air, with no recirculation of air without significant energy penalty due to very low supply air flow rates, and this is achieved without compromise to air change effectiveness due to a high-induction air delivery characteristic. The turbulence, and hence 'mixing' effect caused by this characteristic also promotes a uniform temperature across the space, which is conducive to occupant comfort. Although there appeared to be a high level of 'mixing' in the space, velocities measured in the room were commensurate with good practice. Velocities were <0.25m/s in almost all measured locations, with a much lower average velocity across the occupied zone consistent with ASHRAE 55:1992 recommendations. ACBs also offer the advantage of individual room temperature control. The system will therefore respond to changing loads within each room, which should further improve comfort conditions and allow more scope in the post-occupancy fine-tuning phase of the project.

A number of important lessons have been learned through the modelling and testing process. The CFD model provided confidence that the design decision was appropriate; however, the results were inaccurate in some respects as was shown by the prototyping. The tests showed the importance of accurate CFD modelling of key components. For example, the simplified air delivery characteristic/ steady-state CFD model resulted in understatement of the velocity and turbulence profile in the room. If the inaccuracy had been greater, comfort issues may have otherwise been encountered within the wards post-occupancy. Therefore, the importance of balancing the cost and time imperatives of producing a CFD model against the level of accuracy required, must be carefully considered from the outset, especially if the CFD model is to be the sole basis for design decisions. Consideration should also be given to alternative methods of CFD modelling, especially as hardware and software advances are made. An area for further work is the assessment of improved turbulence and large-eddy-simulation models to more accurately predict velocity profiles for HVAC.

The unique insights that can be gained through full-scale prototyping are clear to see. The approach outlined in this paper is not necessary for most HVAC designs. However, it is most useful for critical or non-standard applications, or where a particular solution is to be repeated many times over and improved quality control or optimisation is required. It should, however be noted that even prototypes have limitations, and actual site conditions, deficiencies in mock-ups, or inaccurate measuring instruments can all lead to a different outcome at the end of the project to that predicted during the tests.

Notwithstanding the limitations, the ability for modelling and prototyping to identify potential improvements was particularly useful for this project. Based on the findings of this study, temperature set-point and humidity control adjustments will be considered prior to the commissioning of the Fiona Stanley Hospital systems to optimise occupant comfort, as well as reduce energy consumption.

The merits of initiating the modelling and prototyping early in the design/ construction process should be considered to allow time to adjust the design, if necessary. Moreover, this re-affirms the need to build appropriate margins and features into HVAC system design to allow for fine-tuning, especially in those designs that are not modelled or prototyped.

ACKNOWLEDGEMENTS

Thanks go to Mike Jennings of AECOM and Mark Pitman for CFD post processing and insights into the results, and Dadanco Pty Ltd for carrying out the prototype room tests and assisting in the analysis.

REFERENCES

ASHRAE 55:1992, *Thermal Environmental Conditions for Human Occupancy*, American Society of Heating, Refrigerating and Air-conditioning Engineers, USA.

Australian Health Insurance Association, 2007, *Hospital Infection Rates too High*, viewed 27 April 2011, http://www.ahia.org.au/media%20releases/AHIA%20Media%20Release%20-%20Hospital%20Infection%20Rates%20Too%20High%202%20Jul%2007.pdf.

BS EN 15116:2008, *Ventilation in Buildings. Chilled Beams. Testing and Rating of Active Chilled Beams*, British Standards Institution, United Kingdom.

BS EN ISO 7730:2005, *Ergonomics of the thermal environment. Analytical determination and interpretation of thermal comfort using calculation of the PMV and PPD indices and local thermal comfort criteria*, British Standards Institution, United Kingdom.

Charles, K.E., 2003, *Fanger's Thermal Comfort and Draught Models*, Institute for Research in Construction, Canada.

Dadanco, 2011, *Test Report – Fiona Stanley Hospital, Perth*, Dadanco, Australia.

Jennings, M., 2010, *Simulation of Turbulent Flow Structures in the Near Wake Region of an Elevated Transverse Jet in Crossflow*, Curtin University of Technology, Australia.

Roth, K., Dieckmann, J., Zogg, R., Brodrick, J., 2007, *Chilled Beam Cooling*, ASHRAE, USA.

Smith, S., Lowndes, P., Wei, L., 2010, *Hospital Energy Performance Benchmarking*, AECOM, Australia.

Figure 2

Ward HVAC design

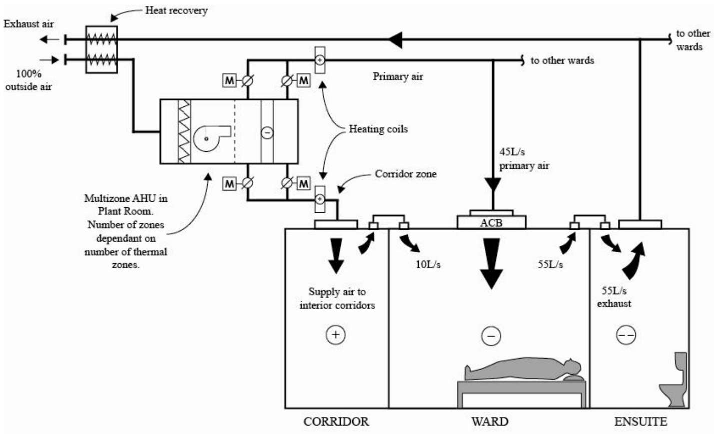

Figure 7

Prototype room layout and measurement point grid (Dadanco, 2011)

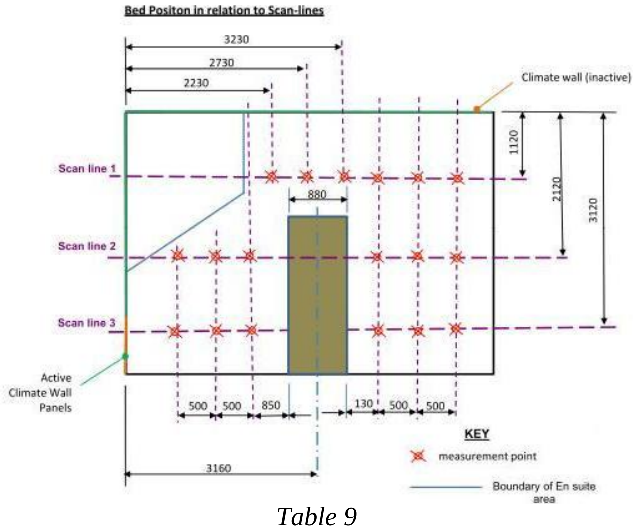

Table 8

Part-load temperature and velocity plots for CFD model (read in conjunction with Figure 7)

MODEL RESULTS									
	Distance (mm)	Temperature (°C)				Velocity (m/s)			
		Height (m)				Height (m)			
		1.7	1.2	0.6	0.2	1.7	1.2	0.6	0.2
Plane 1 (1120 mm)	2230	21.02	21.91	22.43	22.18	0.17	0.08	0.02	0.03
	2730	20.42	23.84	23.89	23.77	0.17	0.05	0.08	0.07
	3230	22.33	23.91	23.80	23.73	0.06	0.07	0.09	0.08
	3730	23.46	23.30	23.22	23.52	0.17	0.13	0.14	0.14
	4230	22.60	23.07	23.00	22.73	0.07	0.11	0.12	0.10
	4730	20.92	22.01	22.01	21.84	0.24	0.11	0.03	0.02
Plane 2 (2120 mm)	870	21.32	21.49	21.59	22.32	0.16	0.07	0.06	0.04
	1370	21.10	22.09	21.85	22.80	0.19	0.02	0.06	0.05
	1870	20.83	22.27	22.21	22.91	0.18	0.04	0.07	0.05
	3730	23.03	22.89	22.17	21.80	0.18	0.10	0.05	0.09
	4230	22.70	22.68	21.90	21.77	0.10	0.05	0.05	0.08
	4730	21.56	22.45	21.92	21.74	0.18	0.09	0.06	0.01
Plane 3 (3120 mm)	870	22.84	22.92	22.52	22.08	0.15	0.03	0.03	0.05
	1370	23.01	23.41	23.43	23.05	0.17	0.05	0.07	0.07
	1870	22.73	23.35	23.53	23.75	0.12	0.03	0.08	0.09
	3730	22.30	22.53	22.43	22.12	0.16	0.03	0.03	0.14
	4230	22.01	22.50	22.31	22.15	0.08	0.05	0.08	0.09
	4730	21.69	22.54	21.95	21.67	0.12	0.05	0.05	0.07

Table 9

Part-load temperature and velocity plots for prototype room (read in conjunction with Figure 7)

ACTUAL RESULTS									
	Distance (mm)	Temperature (°C)				Velocity (m/s)			
		Height (m)				Height (m)			
		1.7	1.2	0.6	0.2	1.7	1.2	0.6	0.2
Plane 1 (1120 mm)	2230	23.24	23.24	23.20	23.30	0.14	0.19	0.20	0.15
	2730	23.34	23.42	23.41	23.47	0.12	0.14	0.12	0.10
	3230	23.51	23.57	23.64	23.64	0.11	0.13	0.13	0.11
	3730	23.57	23.60	23.66	23.63	0.11	0.11	0.12	0.19
	4230	23.58	23.59	23.60	23.51	0.14	0.11	0.09	0.17
	4730	23.55	23.54	23.55	23.51	0.09	0.11	0.08	0.10
Plane 2 (2120 mm)	870	23.15	23.21	23.13	23.07	0.12	0.12	0.16	0.11
	1370	23.16	23.18	23.10	23.05	0.14	0.14	0.13	0.23
	1870	23.17	23.18	23.10	23.10	0.13	0.17	0.13	0.16
	3730	23.20	23.28	23.24	23.28	0.13	0.17	0.21	0.11
	4230	23.28	23.35	23.35	23.30	0.11	0.14	0.11	0.11
	4730	23.41	23.46	23.44	23.35	0.11	0.09	0.06	0.11
Plane 3 (3120 mm)	870	23.18	23.26	23.17	23.06	0.04	0.08	0.14	0.23
	1370	23.22	23.27	23.17	23.06	0.05	0.04	0.12	0.15
	1870	23.26	23.33	23.16	23.06	0.09	0.07	0.12	0.19
	3730	23.28	23.31	23.14	23.00	0.05	0.07	0.07	0.28
	4230	23.29	23.27	23.08	23.04	0.06	0.06	0.16	0.18
	4730	23.29	23.27	23.08	23.04	0.06	0.06	0.16	0.18

Table 10

Part-load temperature and velocity comparison for CFD model and prototype room (read in conjunction with Figure 7)

COMPARISON OF RESULTS									
	Distance (mm)	Temperature (°C)				Velocity (m/s)			
		Height (m)				Height (m)			
		1.7	1.2	0.6	0.2	1.7	1.2	0.6	0.2
Plane 1 (1120 mm)	2230	-11%	-6%	-3%	-5%	19%	-138%	-728%	-485%
	2730	-14%	2%	2%	1%	33%	-184%	-43%	-35%
	3230	-5%	1%	1%	0%	-90%	-85%	-54%	-31%
	3730	0%	-1%	-2%	0%	35%	17%	14%	-34%
	4230	-4%	-2%	-3%	-3%	-117%	-4%	26%	-66%
	4730	-13%	-7%	-7%	-8%	64%	0%	-146%	-321%
Plane 2 (2120 mm)	870	-9%	-8%	-7%	-3%	21%	-59%	-158%	-173%
	1370	-10%	-5%	-6%	-1%	27%	-559%	-113%	-318%
	1870	-11%	-4%	-4%	-1%	28%	-329%	-80%	-234%
	3730	-1%	-2%	-5%	-7%	27%	-71%	-326%	-24%
	4230	-3%	-3%	-7%	-7%	-15%	-176%	-114%	-45%
	4730	-9%	-4%	-7%	-7%	38%	-1%	-8%	-729%
Plane 3 (3120 mm)	870	-2%	-1%	-3%	-4%	75%	-117%	-320%	-404%
	1370	-1%	1%	1%	0%	70%	12%	-67%	-128%
	1870	-2%	0%	2%	3%	28%	-121%	-45%	-120%
	3730	-4%	-3%	-3%	-4%	66%	-91%	-102%	-105%
	4230	-6%	-3%	-3%	-4%	24%	-21%	-94%	-101%
	4730	-7%	-3%	-5%	-6%	48%	-8%	-206%	-182%
		AVERAGE DIFFERENCE			**-4%**	**AVERAGE DIFFERENCE**			**-106%**

Figure 8

Condensation fail test results (Dadanco, 2011)